Nonlinear Final

Rachel St.Clair

December 2019

1 Izhikevich Model of Neuron

Read Reference: Which Model to Use for Cortical Spiking Neurons? by E. Izhikevich. (Click me)

Izhikevich details various computational models of spike (neuron activation) dynamics modeled from information processing. First, he describes spiking behavior in individual biological neurons as neuro-computational features. Each of the 20 features described explain a different neuron ability. I will briefly note a key component of each spiking behavior here, as described in Izhikevich's report. Tonic spiking is observed in three cortical neurons and have a linear relationship with input stimulus. Phasic spiking can signal the detection of an stimulus. Tonic bursting contribute to gamma oscillations. Phasic bursting behave similar to phasic spiking but are more potent due to the bursting activation behavior. Mixed mode refers to single neuron ability to engage in phasic bursting followed by tonic spiking. Spike frequency adaptation is common in neocortical neurons, staring at high frequency tonic spiking and adapting as input persist, perhaps allowing for temporal encoding. Class 1 excitable neurons can fire at low frequency when the input is weak, thus encoding input strength. Class 2 excitable neurons cannot fire low frequency tonic spike and thus do not encode input strength. Spike latency encodes strength of input by delaying onset of spike. Subthreshold oscillations are very common and relate to bandpass filters. Frequency preference and resonance behavior allows neurons to selectively respond to inputs of similar oscillation frequencies. Integration and coincident detection behavior allows neurons without oscillatory patterns to fire at high-frequencies and detect coincident spiking events. Rebound spiking responds to offset of inhibition. Rebound burst, found in thalamo-cortical cells, respond to offset of inhibition with bursting. Threshold variability depends on prior spiking events and may increase or decrease the critical spiking threshold. In bistable neurons, carefully timed stimulus can switch the neuron from resting to tonic spiking. Depolarizing after-potential shorten neuron refractory periods and make such cells hyper-excitable. Accommodation behavior prohibits spiking behavior due to coincidental stimuli. Inhibition-induced spiking and bursting found in thalamo-cortical cells fire due to prolonged hyperpolarization

by inhibitory stimulus.

Izhikevich then details how such behavior can be modelled computationally and effective implementations in terms of floating-point operations per second. He systematically compares 11 different spiking models in their ability to encapsulate the above spiking behaviors and their effectiveness as a complex systems (see Figure 1). Each model has its pros and cons, however as Izhikevich points out, the best model for the task depends on the task to be modelled. Finally, his work uses his own model to create an artificial neural network mimicking biological neuron behavior with computational efficiency, exhibiting many global mammalian brain abilities.

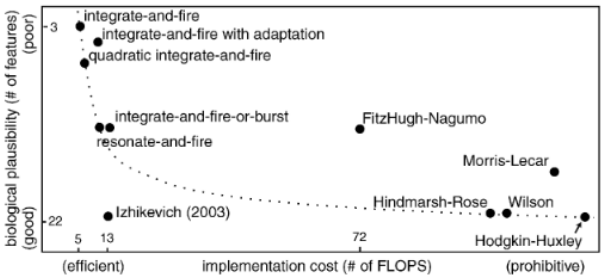

Models	biophysically meaningful	tonic spiking	phasic spiking	tonic bursting	phasic bursting	mixed mode	spike frequency adaptation	class 1 excitable	class 2 excitable	spike latency	subthreshold oscillations	resonator	integrator	rebound spike	rebound burst	threshold variability	bistability	DAP	accommodation	inhibition-induced spiking	inhibition-induced bursting	chaos	# of FLOPS
integrate-and-fire	-	+	-	-	-	-	-	+	-	-	-	-	+	-	-	-	-	-	-	-	-	-	5
integrate-and-fire with adapt.	-	+	-	-	-	-	+	+	-	-	-	-	+	-	-	-	-	+	-	-	-	-	10
integrate-and-fire-or-burst	-	+	+		+	-	+	+	-	-	-	-	+	+	+	-	+	+	-	-	-		13
resonate-and-fire	-	+	+	-	-	-	-	+	+	-	+	+	+	+	-	-	+	+	+	-	-	+	10
quadratic integrate-and-fire	-	+	-	-	-	-	-	+	-	+	-	-	+	-	-	+	+	-	-	-	-	-	7
Izhikevich (2003)	-	+	+	+	+	+	+	+	+	+	+	+	+	+	+	+	+	+	+	+	+	+	13
FitzHugh-Nagumo	-	+	+	-		-	-	+	-	+	+	+	-	+	-	+	+	-	+	+	-	-	72
Hindmarsh-Rose	-	+	+	+			+	+	+	+	+	+	+	+	+	+	+	+	+	+		+	120
Morris-Lecar	+	+	+	-		-	-	+	+	+	+	+	+	+		+	+	-	+	+	-	-	600
Wilson	-	+	+	+			+	+	+	+	+	+	+	+	+	+		+	+				180
Hodgkin-Huxley	+	+	+	+			+	+	+	+	+	+	+	+	+	+	+	+	+		+		1200

Figure 1: Different types of spiking behavior in individual biological neurons, [1]

1.1 Modeling Common Cortical Neurons

Here we will demonstrate models for eight different types of common neurons in mammalian brains, as seen enumerated below, according to Izhikevich's spiking model in python code.

Common types of spiking and bursting neurons:

1. Regular spiking (RS)
2. Intrinsically bursting (IB)
3. Chattering (CH)
4. Fast spiking(FS)
5. Thalamo-cortical (TC) at -63mv
6. Thalamo-corical (TC) at -87 mv
7. Resonator (RZ)
8. Low-threshold spiking (LTS)

In the Izhikevich model of spiking, the behaviors of different cortical neurons can be created by changing parameters a, b, c, and d. The model is represented by two coupled differential equations, $\frac{dv}{dt} = 0.04v^2 + 5v + 140 - u + I$ and $\frac{du}{dt} = a(bv = u)$ where $v \geq +30mV, \{v \leftarrow c$ and $u \leftarrow u + d\}$. In these equations, v represents the membrane potential and u represents the membrane recovery variable accounting for K+ and Na+ ion activation and inactivation, respectively.

Izhikevich Neuron Models in Python Code (Click me)

2 Partial Differential Equations

Read Reference: The Chemical Basis of Morphogenesis by A. Turing. (Click me)

In Turing's introduction to chemical basis of morphogenesis, he attributes biological pattern emergence to the arrival of instability in reaction-diffusion systems. Turing explains how genes determining anatomical structures are subject to some external, mathematically represented, factors. The system can thus be modeled by mechano-chemical states reliant upon position, velocity, elastic and motion stresses, chemical reactions, and chemical diffusion. Morphogens, described as tissue masses where substances are chemically reacting and diffusing, proliferate actions upon the embryo state to illicit anatomical differentiation.

The model system described was subjected to morphogens, initial states that became slightly perturbed due to external influence, and slow changes in the reaction or diffusibility rates to bring about instability. In order to capture the point at which the system become unstable, the linearity assumption (that the system state will not differ to greatly from the original stable conditions) was made. From the onset of instability, morphogen concentrations patterns were observed for six possible cases. I will briefly describe each case here. A) An individual component (cell or part of tissue) drifts from the concentration and reaction rate equilibriums and as it does so influences neighbor components, accounting for dappling pattern (see Figure 2). B) A component experiences drift from the equilibrium in an oscillatory manner. C) An opposite drift from equilibrium from components in contact with each other. D) Wave patterns increasing in amplitude around the components, usually sinusoidal, (see Figure 3). E) A two-morphogen system creating travelling waves (anti-phase in continuous components) (see Figure 4). F) Metabolic oscillation with neighbouring cells in opposite phases.

Figure 2: Dappling pattern on goat.

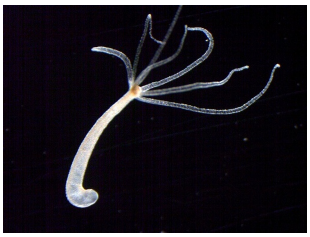

Figure 3: Wave patterns of Hydra.

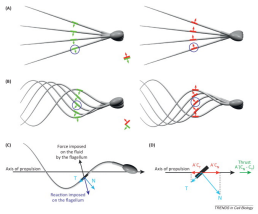

Figure 4: Travelling waves of Spermatozoon tail movement.

Extending these models into growing organisms requires further consideration of the linear assumption. As Turing clarifies, biological organisms are often not growing from the original homogeneous state, but rather from one pattern to the next. For example, a baby goat with one dappling pattern may develop a different dappling pattern as it gets older. In such cases, the next pattern state depends uniquely upon the current pattern state. Although such events extend beyond the mathematical schema presented in this work of Turing's, he contends that these mathematically represented biological conditions can be extended to real-world biological phenomena with the use of non-linear equations.

2.1 Modeling Reaction-Diffusion Systems with Partial Differential Equations

In general, reaction-diffusion systems can be modeled mathematically with partial differential equations. All models of this sort take the general form of initial

state(s) of the chemical(s) perturbed with some small amount of noise, parameters effecting the state(s), update rules dependent on the parameters and laplacian (distance from average neighbor value), and time-step coefficient. The update is performed according the the change in each state provided by the update rule and the laplacian convolution for each time-step. Thus, multiple types of reaction-diffusion equations can modeled by similar functions. Here, we will demonstrate eight different PDE systems as enumerated below.

The 8 PDE systems:

1. - Turing Dappling Morphogenesis (with 2 and 3 morphogens)
2. - Oregonator (modified B-Z rxn)
3. - Wave Equation
4. - Heat Equation
5. - Ginzburg-Landau (nonlinear waves)
6. - Robert Munafo's U-skater (moving shape)
7. - Schenk (dissipative solutions)
8. - Schlogl (bistability)

Reaction-Diffusion PDEs in Python Code (Click me)

3 Systems Biology: Abzyme formation

Read Reference: Modeling in Systems Biology (Click me)

3.1 Problem Description

Many molecular, genetic, and cellular dynamics can be accounted for within models of systems biology. Of such systems is the formation of a complex by two autocatalysing molecules. Since the two molecules, X and Y, are autocatalytic, a positive feedback loop with subsidiary molecules, A and B, determine their available concentrations. In the model proposed by [2], the complex, C, does not effect the change in concentration of X or Y and was left out of the model dynamics. Although Jonsson's model details a single stable fixed point in the system, he attributes this behavior to the set parameters used. Furthermore, the system also defines nullclines, areas of equilibrium. Since this system is of higher dimensionality, there is possibility of oscillations and chatoic behavior, as often seen in natural biological phenomena.

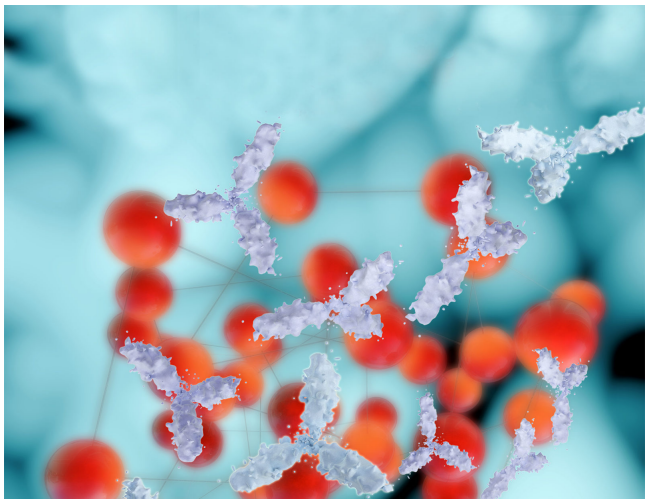

Figure 5: Animated depiction of antibodies (white) forming abzyme complexes with DNA (red).

From this model we can begin to think about an interesting biological application: Abzyme formation. In one of multiple accounts, scientist have found a method of pathogenicity dependent on similar dynamics as described in the autocatalytic complex formation in autoimmune disease [3]. In the case of SLE, the author reports antibodies identifying self-DNA as immune targets. An oligo-pentamer Thymadine repeat on the DNA signals the now autoantibody to bind, which forms a complex called an abzyme (see Figure 5). Since anti-DNA antibodies binding to ssDNA and/or dsDNA and forming abzyme complexes then cause cell death, the formation of the complex cannot be ignored. The antibody will continue binding to snippets of DNA, forming abzyme complexes that are increasingly more rich in DNA. The more DNA bound in the complex, means the more cell death that has occurred. Thus, abzyme formation is a core component of the pathogenic effect. If we adapt the previous model to this proposed dynamical system, we may find interesting methods of prohibiting autoantibody-DNA binding and thus mitigating autoimmune response.

3.2 Simulating Abzyme Complex Formation with Insight Maker

Abzyme formation in the aforementioned model is dependent on autoantibody, X, and ss/dsDNA, Y, concentrations. While, X and Y will be dependent on A, autoantibody reproduction factor, and B, oligo-pentamer repeat synthesizer in DNA. If we view the autoimmune model in this way, we hypothetically allow for antibodies to convert between healthy and auto characteristics, as well as

normal DNA and DNA with the signalling property. Of course, the abzyme complex will be represented by C. Furthermore, we will assume the constant concentrations of subsidiary molecules (or morphogens) are abundant. Upon making these assumption, we can fit the complex interactions of antibody and DNA to a partial differential equation (PDE). Following the example of two autocatalysing molecules that form a complex from [2], the concentration kinetics can be depicted by the equations 1-3 (it should be noted this equations will be the resultant of the model system). Thus the PDE's can be formed by equations 4 and 5 (it should be noted these equations will form the basis of the model system).

$$\mathrm{A} + \mathrm{X} \underset{\mathrm{k_2}}{\overset{\mathrm{k_1}}{\rightleftharpoons}} 2\,\mathrm{X} \tag{1}$$

$$\mathrm{B} + \mathrm{Y} \underset{\mathrm{k_5}}{\overset{\mathrm{k_4}}{\rightleftharpoons}} 2\,\mathrm{Y} \tag{2}$$

$$X + Y \xrightarrow{\mathrm{k3}} C \tag{3}$$

$$\frac{d[X]}{dt} = k_1[A][X] - k_2[X]^2 - K_3[X][Y] \tag{4}$$

$$\frac{d[Y]}{dt} = k_4[B][Y] - k_5[Y]^2 - K_3[X][Y] \tag{5}$$

Implementation of this system is illustrated in application Insight Maker below.

Abzyme Formation Insight Maker here (Click me).

3.3 Simulating Abzyme Complex Formation in Python

Implementation of the PDE system in python is accessible at the link below. As we can see in the figures produced by the simulation bellow, the changes in concentration of the morphogens react proportionally to one another. This is expected since the concentrations of both X and Y are ruled by nearly identical kinetics, with subsidiary morphogens A and B differing (see Figure 6). The complex formation, C, slowly increases in the beginning of the model as concentrations of X and Y are growing, until the system becomes saturated (see Figure 7). At the point of saturation, complex formation become exponential. Since this is an open system, the model does not account for the limited space a more realistic implementation would have (ie. in a cell). Multiple modifications to the current computational model would need to account for the assumptions and limitations aforementioned, but is foreseeable as basic scientific research on the subject and computational algorithms become more advance.

Autocatalytic Complex Formation in Python (Click me).

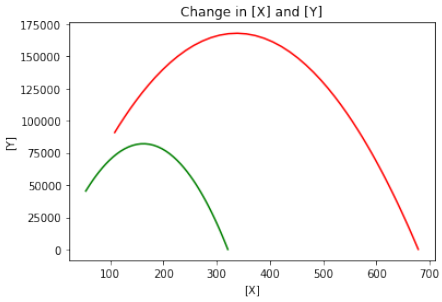

Figure 6: Changes in concentration amongst autocatalytic morphogens, X (red) and Y (green).

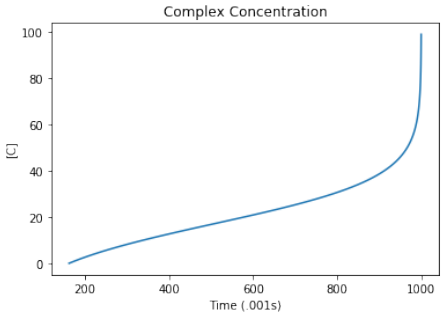

Figure 7: Complex formation as the two chemical, autocatalytic model is simulated over time.

References

[1] E. M. Izhikevich, "Which model to use for cortical spiking neurons?," *IEEE transactions on neural networks*, vol. 15, no. 5, pp. 1063–1070, 2004.

[2] H. Jonsson, "Lecture notes in systems biology," pp. 7–10, 2012.

[3] P. C. Swanson, C. Ackroyd, and G. D. Glick, "Ligand recognition by anti-dna autoantibodies. affinity, specificity, and mode of binding," *Biochemistry*, vol. 35, no. 5, pp. 1624–1633, 1996.